Study of the Influence of Metal Surface Quality on the Performance of an Epoxy Coating

Naima Boudieb[*1,2], Moussa Bounoughaz[1,2], Zohra Ghebache[3] and Fahim Hamidouche[1,2]

[1]*Facultyof Sciences, Department of Chemistry, M'hamed Bougara University of Boumerdes, Algeria*
[2]*Laboratory of Treatment and Formation of Fibrous Polymers, Faculty of Technology, M'hamed Bougara University of Boumerdes,Algeria*
[*]Corresponding author: n.boudieb@univ-boumerdes.dz

Received 25/02/2023; accepted 15/04/2023
https://doi.org/10.4152/pea.2024420501

Abstract

In the present work, an EC used for steel corrosion protection was characterized by Ec techniques. This study aimed to describe the effect of the steel roughness surface on the performance of EC, through EIS and other methods. The studied metal was a low-strength CS immersed in a 3.5% NaCl solution. The CS surface was obtained by polishing it (metal electrodes) with an abrasive paper of 120, 600 and 1200 mesh. Then, the electrodes were painted with an anti-corrosive EC, which contained $Zn_3(PO_4)_2$ as an anti-corrosion agent. The study of the influence of the CS surface R_a and its corrosion behaviour and of the evolution of the protective capacity systems on the EC performance was made by stationary (E_{corr} and Tafel plot) and no-stationary Ec techniques (EIS and CA). In order to confirm the detachment and blistering on the coating, the coated CS samples were analyzed by a salt spray in a 7.69 % NaCl solution, with an IT of 15 days. The obtained results showed that the CS surface state directly influenced the coating performance and the Ec parameter values variation, as a function of IT in the NaCl solution. EIS was the most valid Ec method for the studied coatings.

Keywords: corrosion; CA; EIS; EC; surface roughness; Tafel plot.

Introduction[•]

Corrosion is an extremely crucial problem that is of concern in many different applications for oil production. Corrosion is mainly caused by the conveyed fluids diversity, the variety of materials used, the equipment ageing and, more particularly, the performance of the coating protection [1, 2].

The passive protection of the metal installations against corrosion is ensured by metallic or organic coatings such as anti-corrosive EC and varnishes. The use of organic coatings is one of the most efficient and economical used methods to protect metals. Organic coatings limit the flow of the aggressive elements by creating a physical barrier. Most coatings are not perfect, and consequently, the metal contact with the corrosive medium is inevitable. The coating barrier

[•] The abbreviations and symbols definition lists are in pages 324-325.

properties are linked to various intrinsic parameters, such as its thickness, polymer matrix, fillers, pigments, additives, solvent, adherence, and chemical composition (metal/coating interface). It is acknowledged that water absorption onto coatings is an important topic [3, 4], because it is an initial step in their degradation process. A painting is a fluid preparation that can be spread out in thin layers over all kinds of materials (called supports) to form (hardening) a thin coating, after drying or reticulation. In their design, paintings are a particular composite material, since they generally comprise many compounds (resins, solvents, pigments, loads and additives), which confer them specific physico-chemical properties. Solvents are the most common compounds used in paintings.

Barrier property of an organic coating, for the corrosion protection of metallic substrates, is a loosely defined concept that encompasses, depending on the authors: low permeability to water and O, even if all polymers usually absorb water to various extents, depending on their chemical composition; IT prevention of exposure to water and O at the metal/coating interface (wet adhesion); and limitation of electrical i_{corr}, due to high electrical resistivity in the coating [5-11].

Generally, a protection system by paintings consists of several layers, each of them with a precise purpose. It includes a primary, one layer or several intermediate ones and a top coat. Corrosion resistance of the covered steel structures is strongly influenced by their surface quality. This is why surface preparations of materials, specially polishing operations, are crucial, since they allow to modify their properties. After these treatments, the surfaces become very active [12-15].

This study aimed to investigate the effect of CS surface roughness on the performance of EC currently used for corrosion protection by stationary and non stationary Ec methods, and to assess the corrosion behaviour of CS covered by a painting EC in three surface states immersed in a 3.5% NaCl solution. Several Ec techniques were used: E_{corr} (follow-up of E, according to IT), Tafel method, cathodic delamination test (CA) and EIS. EIS took a large part in this study, as it is widely used for the assessment of organic coatings barrier properties. The impedance response of an organic coating is generally monitored over IT in an electrolytic solution, representative of the operating environment. This monitoring serves to detect the appearance of corrosion signatures in the impedance spectra, hence predicting the coating lifetime. The coating performance is generally evaluated through parameters extracted from equivalent circuits, the physical origin of which is often debatable. The only test that does not belong to the Ec method is salt spray, which was carried to complete the results obtained by the various Ec techniques.

Experimental protocol

Samples and application

EC have been chosen for this study, since they are generally recognized for their higher adherence, good corrosion and unsticking resistance under cathodic polarization, which could explain why they are currently employed by certain gas and oil companies throughout the world [16-20].

The coatings preparation method was performed by selecting $Zn_3(PO_4)_2$, an anti-corrosive agent, as primary layer. The selected coating was a bi-component system

painting: the base was a liquid EC that was homogeneously mixed with the hardener and an appropriate amount of polyamido-amine (versamid type) resin curing agent with different additives. The samples were prepared at ENAP, Lakhdaria, Algeria.
Table 1 presents the coating formulation composition, and Table 2 shows the principal products incorporated in the anti-corrosive primary formulations.

Table 1: Centesimal formula of the coating.

Components	wt%
EC	51
Loads	30
Additives	0.3
Mix solvents	18.7

Table 2: Principal products incorporated in the primary.

Composition	wt%
EC	30.5
Anti-corrosive agent ($Zn_3(PO_4)_2$)	7.5
Pigments	21
Loads	19.5
Additives	5.7
Mix solvents	15.8

The films were deposited on CS electrodes. The painting application was carried out by an air gun with de-oiled air, dehydrated, vacuum-cleaned and compressed with a pressure of 2.5 bar, in an application cabin. The samples were simply degreased with xylene, then polished manually by using abrasive silicon carbide paper, and finally rinsed with acetone.
The films thickness values obtained after drying (in the air), were measured using a magnetic thickness gauge positector 2000. The painted system was composed by a primary layer and a top coat of 25 $\pm$3 and 25 $\pm$ 3 µm, respectively.
The covering time between the primary and the top coat was 48 h, to ensure physical and chemical hardening.
The EC were conditioned for, at least one week, at 23$\pm$2°C and 50$\pm$10% of relative humidity, before Ec measurements. These conditions were required for the pores opening, since, without them, the coating would act as an insulating physical barrier, hindering the presence of curves in Ec measurements.

EIS
A standard cell with three electrodes was used: WE was a CS coupon, with a surface of 32cm^2; RE was a SC and AE was Pt. The electrodes were connected to the measuring equipment (EGG Mode l 273A potentiostat/galvanostat, with three entries).
The testing solution was 3.5% NaCl. Impedance measurements were carried out with a response frequency recorder from10^5 Hz to 1 mHz, with 5 points per decade.

Polarization curves

In order to plot the polarization curves, PDP measurement, with a E variation of ±250 mV vs. E_{corr}, at a SR of 0.166 mV/s, was performed. This test was carried out only once, at the start of the coating steel immersion on a separate layer.

CA

CA consists in following I evolution vs. time, when the system is subjected to overpressure. Herein, cathodic delamination test was used, which consists in imposing on the electrode a E lower than its E_{corr}, and measuring i_{corr} vs. time. This test allows to evaluate the coating performances over time, under cathodic protection.

In order to simulate real conditions, all steel coatings were scratched until the metal surface appeared (coating surface scratch: 2 cm × 2 mm). Imposed E was 1.2 V/E_{corr}.

Experimental results

Study of bare metal

Reduction E

The follow-up curves of the free E during the bare metal corrosion, for three studied R_a values are presented in Fig. 1. Whatever the considered surface R_a, E decreased, since the immersion started from a noble value to a stabilized one located from-700 to -750 mV/SCE. The following values resulted from several tests: 1 (120 mesh) = -746 mV/SCE; 2 (600 mesh) = -719 mV/SCE; 3 (1200 mesh) = -708 mV/SCE.

E became progressively less noble (Fig. 1) at the immersion beginning. There was a continuous attack on CS, and the free E stability shows that the systems that went through the corrosion process had the same kinetics during the samples immersion in NaCl [21].

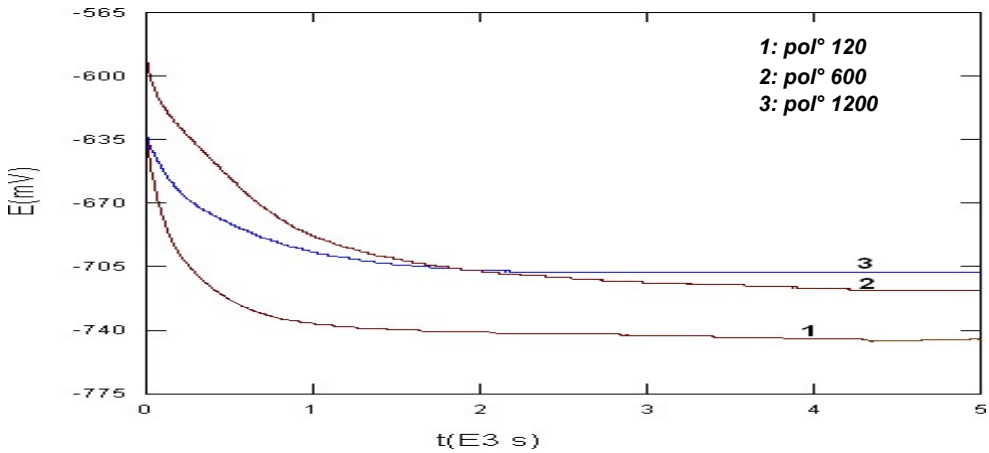

Figure 1: Follow-up of the free E of bare metal in NaCl 3.5 % for the three samples surface R_a.

Polarization curves

In order to determine Ec parameters for corrosion evolution, PDP plots were performed on the bare CS samples, at various surface states. Polarization curves were obtained by scanning E from +250 mV around free E. E scanning was done

from the cathodic to the anodic field, at the SR of 0.166 mV/sec. This type of curve allowed determining I_{corr} and E_{corr}. Fig. 2 represents polarisation curves obtained for the bare CS electrodes, in aerated conditions, for the three surface states. Measurements were done after free E stabilization. E_{corr} and j values were obtained by the polarization curves (extrapolation method of Tafel lines). Ec parameters values obtained from these curves are shown in Table 3.

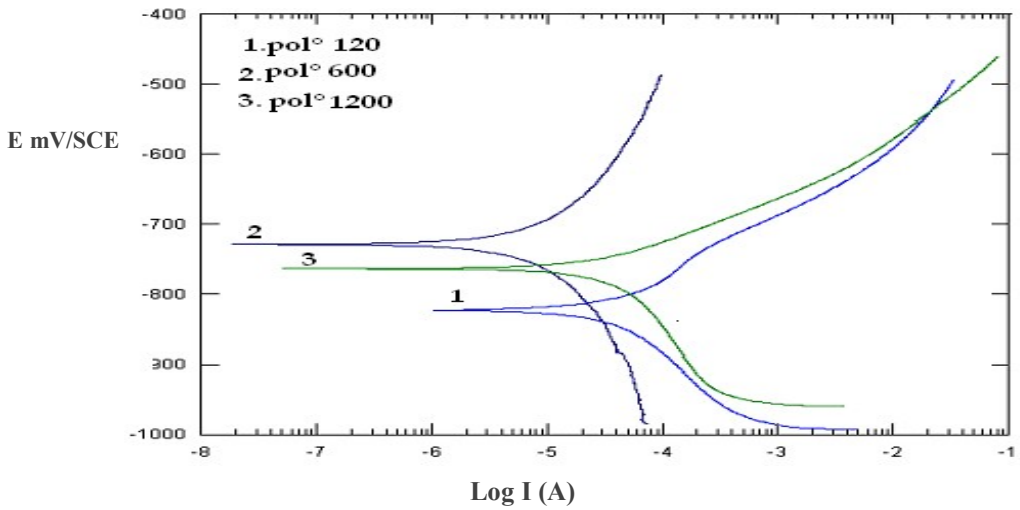

Figure 2: Polarization curves of bare metal at various surface state sin a 3.5% NaCl medium.

Table 3: Ec parameters values obtained from polarization curves.

Mesh	E_{corr} (mV/SC)	I_{corr} ($\mu A/cm^{-2}$)
120	823.1	37.96
600	728.0	25.46
1200	764.2	39.54

Polarization curves (Fig. 2) show that the surface state influenced E and J. It should be noted that E_{corr} shift in the negative direction of approxim. 58.9 mV/E for the surface polished at 120 mesh vs. CSE was compared to the surface polished at 1200 mesh. J values were larger for the electrodes polished at 120 and 1200 mesh, than for the one polished at 600 mesh.

EIS

EIS was successfully applied for the study of CS corrosion mechanisms. EIS diagrams in Nyquist and Bode representation of bare metal obtained for various studied R_a values are shown in Fig. 3.

C_{res} and C_{rev} results obtained from these curves are shown in Table 4. Whatever the surface state, the impedance diagram was composed of a loop in the low frequencies field that reported corrosion phenomena at CS/electrolyte interface.

In Bode plot, impedance diagrams show the presence of only one time constant at low frequencies. Concerning the impedance phase, diagrams loops are similar for the three considered surface states.

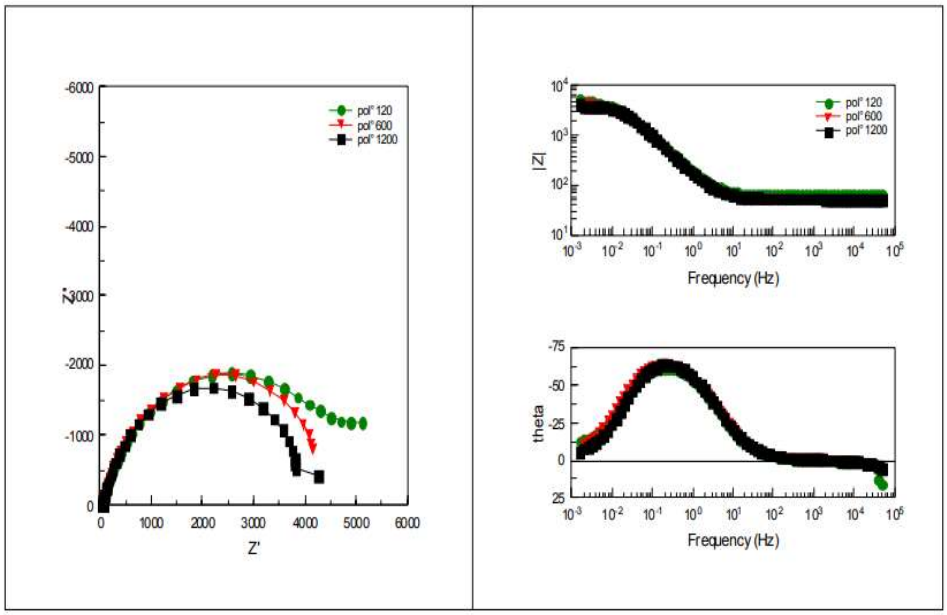

Figure 3: Impedance diagrams in the complex and Bode plan of bare CS in 3.5% NaCl, for the three surface states.

Table 4: Electric parameters of the metal-solution interface obtained during CS immersion in 3.5% NaCl.

Mesh	R_p (Ω)	C_{dl} (Farads)
120	5148.9	$194.35 .10^{-5}$
600	4590.0	$222.16 .10^{-5}$
1200	3281.2	$201.79. 10^{-5}$

R_p values recorded after polishing with abrasive paper of grades 120, 600 and 1200 mesh, respectively (Table 4), show that they increased in the order: R_p (1200 mesh) < R_p (600 mesh) < R_p (120 mesh). One also noted an increase in the capacity with a decrease in C_{res} value. R_p decreased with increased C_{rev} values. This behaviour was due to the increase in the corroded CS surface.

Study of the coating

E_{corr}

E_{corr} curves vs. IT of CS samples for the studied surface states are shown in Fig. 4. E_{corr} shifted towards the negative direction after two days IT. Then, it shifted towards the noble direction, and finally moved towards the negative direction, until the experiment end, at 91 days. E displacement towards the noble direction indicates that the cathodic/anodic reactions ratio increased, and both O and water penetrated the coating, reaching the CS/coating interface. E shift towards more negative values indicates that the anodic/cathodic reactions ratio became significant. The increase in E_{corr} towards higher positive values over time, indicates that alkaline conditions were locally developed at the CS/coating interface. E_{corr} displacement towards increasing negative values over time indicates the formation of corrosion products, and the limited coating service life [22, 23].

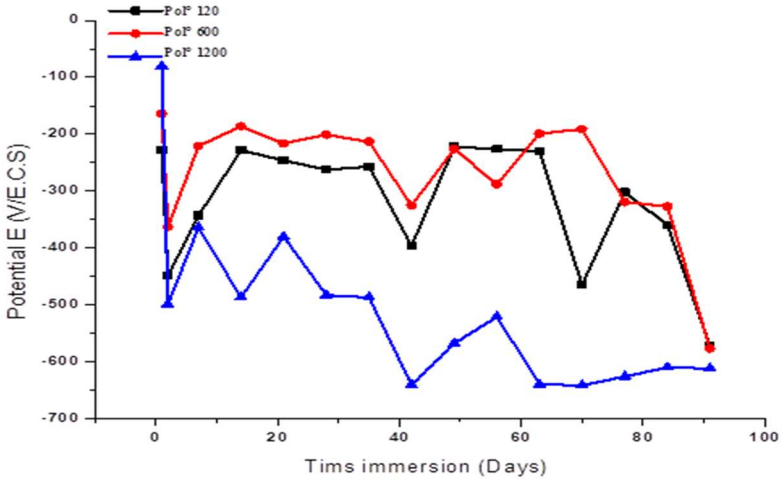

Figure 4: Follow-up of E_{corr}during CS immersion in a NaCl 3.5 % medium, at different surface states.

EIS

Low frequency impedance modulus (1 MHz) is commonly used to evaluate the overall anti-corrosion performance of organic coatings [24-27]. Figs. 5, 6, 7 and 8 present the impedance diagrams evolution, during IT of CS in the 3.5 % NaCl solution for the EC, at different R_a values.

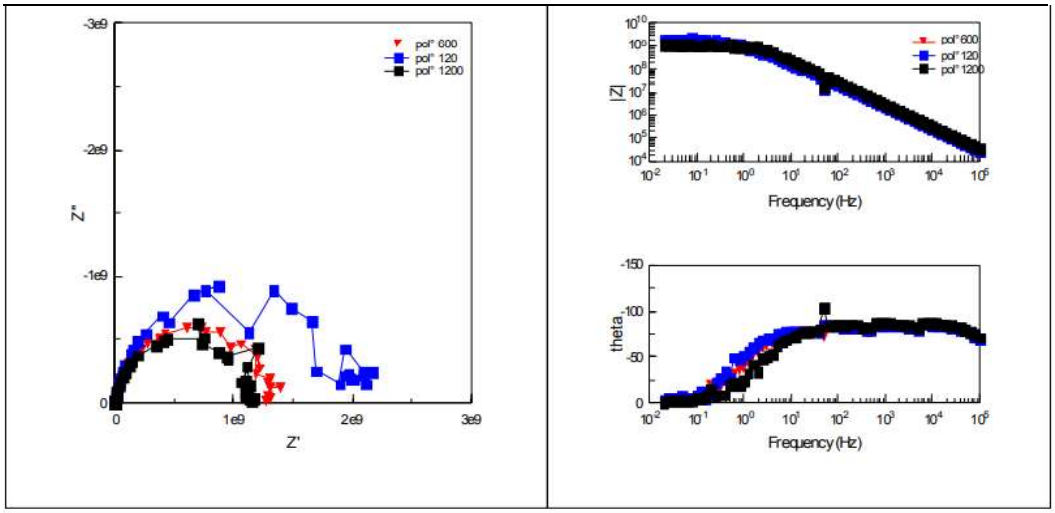

Figure 5: Impedance diagrams of the system in 3.5% NaCl after 2 days IT.

A collapse of the impedance was observed from 2 to 7 days IT, for the three R_a values ($10^9 \rightarrow 10^8 \Omega$). Then, for longer IT, the impedance diagrams remained relatively stable around average values ($1.77.10^8$, $1.44.10^8$ and$1.16.10^8\ \Omega$, for 120, 600 and 1200 mesh, respectively). Thus, the metal/coating system resisted corrosion. At the end of IT (86-91 days), impedance had a visible evolution, but it was still significantly lower ($10^7\Omega$). C_{rev} value was estimated at $C = 10^{-11}$ F/cm^{-2}, which is characteristic of an organic coating [28].

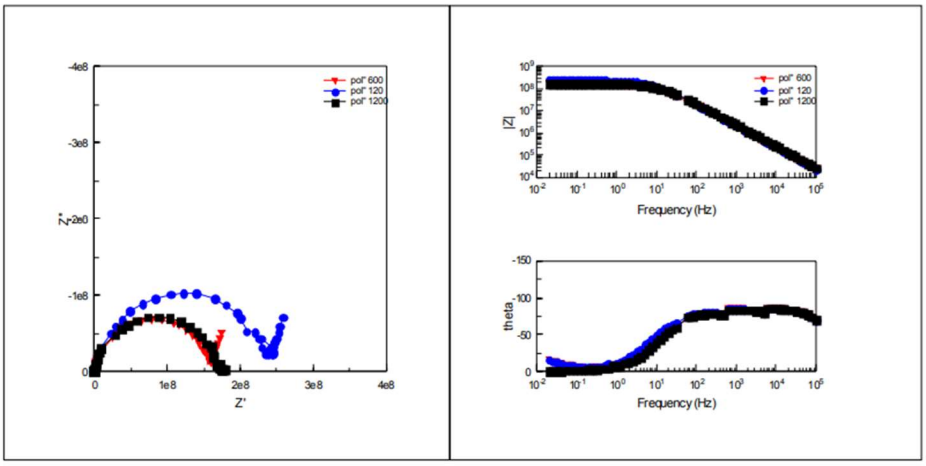

Figure 6: Impedance diagrams of the system in 3.5% NaCl after 35 days IT.

Impedance diagrams are characterized by two time-constants: high frequency field, which represents the coating properties, and low frequency field, which is attributed to phenomena occurring at depth in the paint pores.

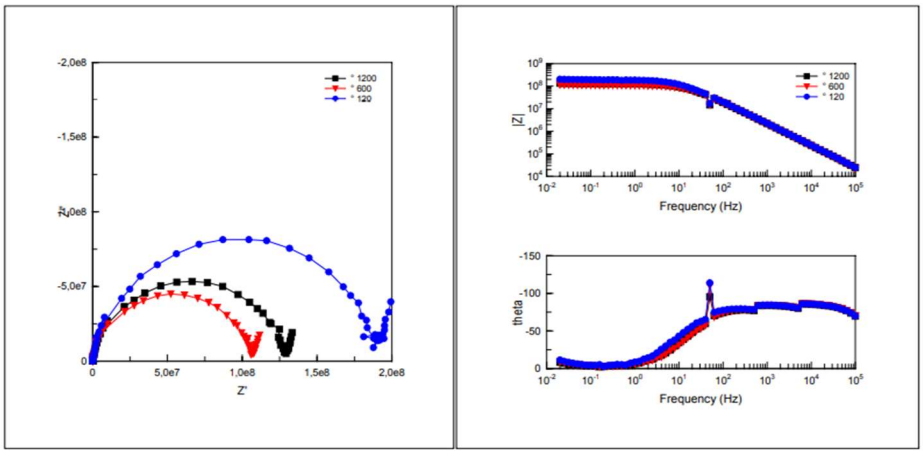

Figure 7: Impedance diagrams of CS/coating in 3.5% NaCl after 77 days IT.

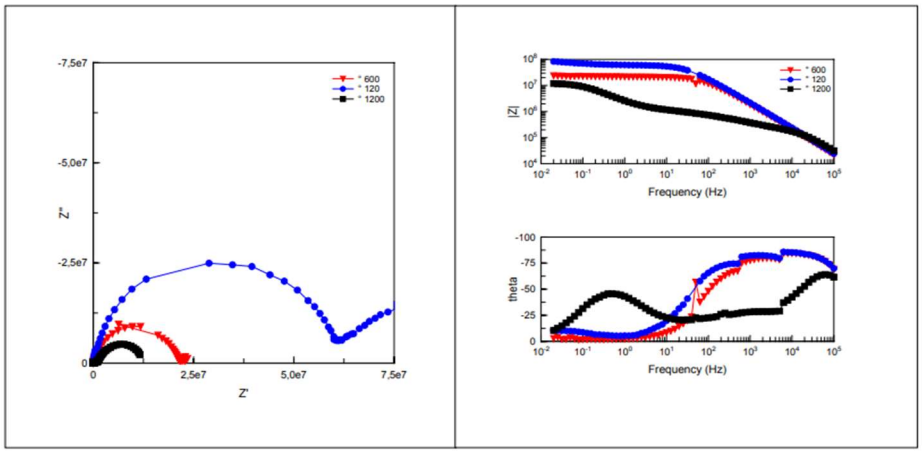

Figure 8: Impedance diagrams of the metal/coating in 3.5 % NaCl after 91 days IT.

R_p and C_{rev} values were extracted from Ec impedance diagrams, in order to assess changes in the coating properties with IT. Fig. 9 represents the evolution of R_p values extracted from the high frequencies loop, which characterizes the EC effect of the three electrodes on the surface states. The systems R_p and C_{rev} values are shown in Tables 5 and 6, respectively.

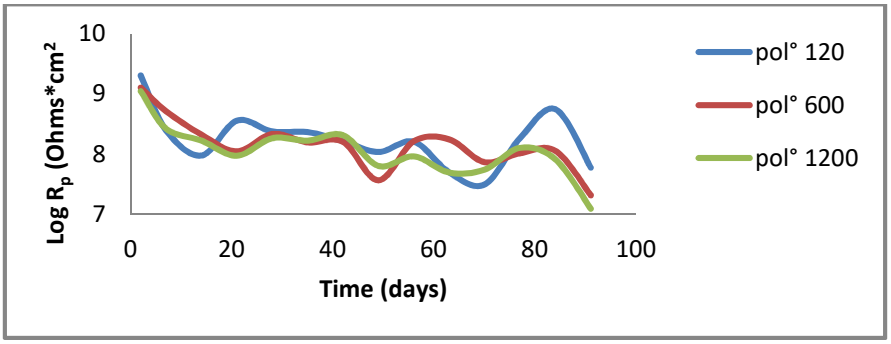

Figure 9: Evolution of R_p values extracted from high frequencies loop vs. IT.

Table 5: R_p values vs.IT.

Mesh	IT (days)	2	7	14	21	28	35	42	49	56	63	70	77	84	91
120*	R_p 10^8 (Ω/cm^2)	20.05	2.54	0.92	3.71	2.43	2.39	1.68	1.10	1.64	0.51	0.33	1.91	0.57	0.62
600*		13.27	5.28	2.15	1.43	2.32	1.60	1.65	0.37	1.66	1.79	0.76	1.07	1.16	0.21
1200*		11.41	2.70	1.70	0.97	1.88	1.71	2.12	0.65	0.94	0.49	0.57	1.30	0.83	0.13

Table 6: C_{rev} values vs.IT.

Mesh	IT (days)	2	7	14	21	28	35	42	49	56	63	70	77	84	91
120*	$C_{rev}*10^{-10}$ (F/cm^{-1})	1.12	1.09	9.90	1.09	0.95	1.01	1.09	1.02	0.92	0.84	0.95	0.92	0.83	0.87
600*		1.04	1.18	1.20	0.97	0.94	1.00	1.06	2.10	0.99	1.08	1.09	0.95	1.14	1.23
1200*		1.53	1.23	0.86	1.01	0.88	0.86	0.69	3.31	1.99	0.86	0.56	0.08	0.88	1010

According to Fig. 9, for the electrodes polished with 120 and 600 mesh, C_{res} values decreased in the first IT, then stabilized. This shows that, due to the system adhesion, corrosion protection remained rather significant and constant for a relatively long IT. At the end of the experiment (70-91 days), one noticed a decrease in C_{res} that was due to the electrolyte penetration in EC pores, which put CS in direct contact with NaCl.

Concerning the electrode polished with 1200 mesh, C_{res} values decreased with IT, and were weaker than those observed for the other electrodes. This evolution was accompanied by an increase in C_{rev} values. R_p and C_{rev} evolution was due to the increase in the corroded MC surface under EC, which led to the formation of an oxides layer.

The increase in C_{res} during IT can be explained by the following phenomena: corrosion products growth on the material surfaces (in EC pores) had a barrier effect which slowed down CR; the localised character of corrosion involved a reduction in EC active surface, artificially inducing an increase in R_p; and the decreased medium aggressiveness related to the increase in pH, which involved a

deceleration in CR. Whatever the surface state, R_s value in EC pores decreased, due to their enlargement and hydration during IT.
According to this evolution, electrodes polished with120 and 600 mesh showed a better barrier effect against the electrolyte than the one polished with 1200 mesh. C_{rev} values (Table 6) remained relatively stable over IT of the three polished electrodes (120, 600 and 1200 mesh). Stable or slightly increased C_{rev} values were due to the solution saturation and accumulation in EC and under it [27].
For longer IT, C_{rev} values of the electrode polished with1200 mesh tended to increase, which agrees with various researches that employed Ec impedance measurements to study metals coatings degradation. Thus, due to the aggressive medium high polarity, the system dielectric constant and C_{rev} increased, as written in eq. (1).

$$C=\xi_o\xi_r S/e \quad (1)$$

Absolute permittivity is the medium property that reveals the flux density generated at a given point, due to a certain electric field intensity at another point in that field. The increased ξ_r constant value involved higher C_{rev} values [29, 30].
R_p values decreased significantly during the first 7 days IT, due to EC non-destructive delamination. Then, a relative R_p stability occurred for longer IT. Finally, a reduction in R_p happened due to EC detachment.

Test of cathodic delamination
To protect steel structures, such as underground pipelines, cathodic protection is used in conjunction with organic coatings. However, these later deteriorate with time. In addition, combining a cathodic protection with an organic coating causes a high alkalinity at the coating/steel interface, resulting in coating cathodic disbondment. As a result, more electric power is consumed over time, and the steel structure is preserved. In the end, E demand may surpass the protection system designed capabilities [29-33]. Herein, the protective E imposed on EC tested in different surface states was checked in order to assess its detachment. Fig. 10 shows EC amperometric curves for the three surface states.

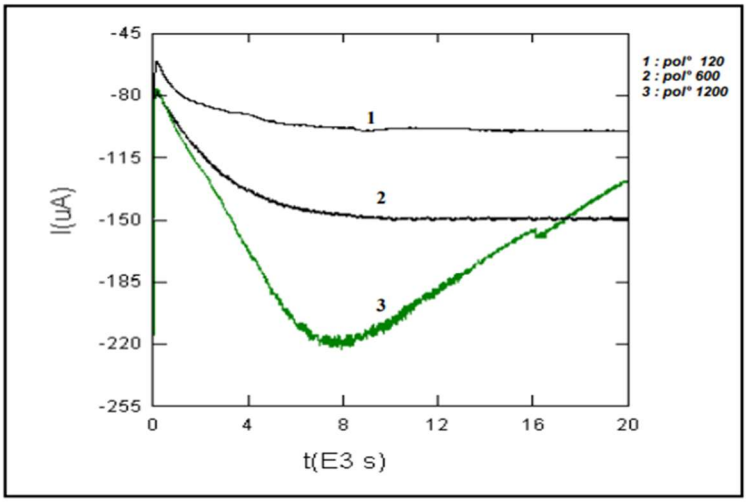

Figure 10: CA curves of CS/ EC for the three electrodes.

The amperometric curve corresponding to EC of the electrode polished with 1200 mesh had lower C_{res} for CS undercoating cathodic protection, because I increased from -218 to -125 µA. This did not happen with the other electrodes (600 and 120 mesh), of which cathodic I remained practically stable. As such, organic EC are incompatible with E cathodic protection.

It should be noted that EC with various R_a values underwent a cathodic delamination test for an overprotection of approxim. -600 mV/SCE, knowing that $E_{applied}$ - E_{corr} = -1200 - (- 600) mV/SCE.

It was seen that the tested systems were not degraded, since neither delamination nor blisters formation occurred around the scratches. This shows that EC systems adhered well on CS. However, the surface polished with 1200 mesh was almost mirror-like. Therefore, the coating detachment was easier.

Salt spray test

A salt spray test was carried out to complete the results obtained by various Ec techniques. This is an accelerated corrosion test generally defined as a method that enables to evaluate coatings performance, and of which results are obtained with shorter IT than those of natural exposure.

In this work, the solution was 7.69% NaCl, and room temperature was 35 ºC. IT was 15 days. The saline solution was periodically added after every 80 h. Blisters formation and CR of the EC metal plates were regularly evaluated by visual observations. Samples photographs were taken after 15 days IT, in salt spray. Fig. 11 shows that the primer formulated with EC 1200 mesh had better anti-corrosion performance. The blisters are spaced apart, and their diameter is much smaller than those of the primer formulated by $Zn_3(PO_4)_2$, with 600 and 120 mesh, which are more numerous and close together.

Figure 11: Salt spray test, with an IT of 15 days.

Conclusion

A study on the influence of the substrate R_a was carried out by Ec techniques. The objective was to establish a link between the interface morphology (of the surface state) and the coating adhesion. Ruled by the bindings generated between CS and the deposited EC layer, adhesion results from physical and chemical bonds

between the former and the latter. Two elements influenced EC adhesion: its microstructure and the interface morphology.
E_{corr}variations with IT showed that CR of CS increased with its lower surface R_a (increase in the anodic/cathodic surfaces ratio).
Non-optimized paint application parameters led to porosities and low plastic deformation of EC and CS, i.e. a non-ideal coating microstructure. In this case, the interface rupture was facilitated, and adhesion level was low. The interface morphology was, in turn, ruled by R_a of CS before EC application. EC particles capture associated with their lower rate of penetration into CS was higher, thus increasing the system surface. EC-based $Zn_3(PO_4)_2$ protected CS through passivation by shifting E towards more electropositive values than those of the bare metal. Ec impedance measurements allowed to quickly evaluate parameters that agreed with what was observed using stationary methods. C_{res} and C_{rev} measurements enabled to assess EC corrosion resistance brought by the anti-corrosive pigment.
EC did not detach during delamination tests, which shows that the system adhered well on CS. Thus, EC can be considered as good protection systems for metal structures in saline and aggressive media. Finally, Ec tests enabled to highlight a correlation between the interface morphology and the adhesion level. A higher CR was obtained for rough interfaces (600 mesh), and compared to other experimental results (salt spray test).

Acknowledgments
The authors would like to express their sincere appreciation to M'hamed Bougara University of Boumerdes for all support. Special thanks are also extended to Laboratory of Treatment and Formation of Fibrous Polymers that helped in the completion of this study.

Authors' contributions
Naima Boudieb: collected the data; inserted data or analysis tools; performed the analysis; wrote the paper. **Moussa Bounoughaz**: conceived and designed the analysis; inserted data or analysis tools; performed the analysis; wrote the paper. **Zohra Ghebache**: wrote the paper. **Fahim Hamidouche**: realized salt spray test observations and interpretation of their results.

Abbreviations
AE: auxiliary electrode
CA: Chronoamperometry
C_{dl}: double layer capacity
CR: corrosion rate
C_{res}: coating resistance
C_{rev}: coating capacity
CS: carbon steel
e: coating thickness
E: potential
Ec: electrochemical

EC: epoxy coating
E_{corr}: corrosion potential
EIS: electrochemical impedance spectroscopy
ENAP: *Enterprise national algérienne des peintures* (Algerian national painting company)
I: current
I_{corr}: corrosion current
IT: immersion time
J: current density
PDP: potentiodynamic polarization
RE: reference electrode
R_p: polarization resistance
R_s: solution resistance
S: exposed surface
SCE: saturated calomel electrode
SR: scan rate
WE: working electrode
$Zn_3(PO_4)_2$: zinc phosphate

Symbols definition
ξo: vacuum permeability
ξ: medium absolute permittivity
ξr: coating relative permittivity

References

1. Cambruzzi A, Rossi S, Deflorian F. Reduction on protective properties of organic coatings produced by abrasive particles. Wear. 2005;258:1696-1705. https://doi. org/10.1016/j.wear.2004.11.023
2. Roggero A, Villareal L, Caussé N et al. Correlation between the physical structure of a commercially formulated epoxy paint and its electrochemical impedance response. Prog Org Coat. 2020;146:105-729. https://doi.org/10.1016/j.porgcoat.2020.105729
3. Fernández-García M, Chiang MYM. Effect of hygrothermal ageing history on sorption process, swelling, and glass transition temperature in a particle-filled epoxy-based adhesive. J Appl Polym Sci. 2002;84:1581-1591. https://doi.org/ 10.1002/app.10447
4. Nogueira P, Ramírez C, Torres A. Effect of water sorption on the structure and mechanical properties of an epoxy resin system. J Appl Polym Sci. 2001;80:71-80. https://doi.org/10.1002/1097-4628(20010404)80:13.0.CO;2-H
5. Veselý D, Kalendová A, Němec P. Properties of organic coatings depending on chemical composition and structure of pigment particles. Surf Coat Technol. 2010;204:12-13. https://doi.org/10.1016/j.surfcoat.2009.11.005
6. Arrieta A, Barrera I, Mendoza J. Polyaniline as Additive to Improve the Anticorrosive Properties of Commercial Paint. Rev Chim. 2021;72(3). https://doi.org/10.37358/rc.21.3.8444
7. Assassi F, Benharrats N. Synthesis, characterizations and application of polyaniline-paint as anticorrosion agent. Inorgan Nano-Metal Chem. 2021;51(6). https://doi.org/10.1080/24701556.2020.1810707

8. Jašková, V, Kalendová A. Anticorrosive coatings containing modified phosphates. Progr Org Coat. 2012;75(4). https://doi.org/10.1016/j.porgcoat.2012.07.019
9. Sangaj NS, Malshe VC. Permeability of polymers in protective organic coatings. Prog Org Coat. 2004;50:28-39. https://doi.org/10.1016/j.porgcoat.2003.09.015
10. Wicks ZW, Jones FN, Pappas SP et al. Corrosion protection by coatings. Org Coatings. John Wiley & Sons. Inc., Hoboken, NJ, USA. 2007:137-158. https://doi.org/10.1002/9780470079072.ch7
11. Leidheiser H. Electrical and electrochemical measurements as predictors of corrosion at the metal-organic coating interface. Prog Org Coat. 1979;7:79-104. https://doi.org/10.1016/0300-9440(79)80038-7
12. Kalendova A, Kalenda P. The study in anticorrosive pigments based on modified phosphates. Lakokrasochnye Materialy i Ikh Primenenie. 2004.
13. Liu S, Dong Z, Wang XZ et al. Different acid doped polyaniline waterborne epoxy coatings: Anticorrosion and passivation performance on 5083 Al alloy. Prog Org Coat. 2022;173:107-182. https://doi.org/10.1016/j.porgcoat.2022.107182
14. Gergely A, Bertóti I, Török et al. Corrosion protection with zinc-rich epoxy paint coatings embedded with various amounts of highly dispersed polypyrrole-deposited alumina monohydrate particles. Prog Org Coat. 2013;76(1):17-32. https://doi.org/10.1016/j.porgcoat.2012.08.005
15. Roggero A, Villareal L, Caussé N et al. Correlation between the physical structure of a commercially formulated epoxy paint and its electrochemical impedance response. Prog Org Coat. 2020;146:105-729. https://doi.org/10.1016/j.porgcoat.2020.105729
16. Navarchian A, Joulazadeh H, Karimi F. Investigation of corrosion protection performance of epoxy coatings modified by polyaniline/clay nanocomposites on steel surfaces. Prog Org Coat. 2014;77(2). https://doi.org/10.1016/j.porgcoat.2013.10.008
17. Deshpande P, Kolekar A, Bhopale A et al. Impressed current cathodic protection (ICCP) of mild steel in association with zinc based paint coating. Mat Tod Proceed. 2021;50:1660-1665. https://doi.org/10.1016/jmatpr. 2021.09.145
18. Charles G, Munger L, Vincent D. Corrosion Prevention by protective coatings. NACE international, Second edition, USA, 1999:317-338.
19. Von Fraunhofer JA, Boxall J. Protective Paint Coatings for Metals. 1976;67. Portcullis Press Ltd, Surrey, U.K
20. Zhang L, Lu X, Zuo Y. The influence of cathodic polarization on performance of two epoxy coatings on steel. Int J Electrochem Sci. 2014;9:6266-15280.
21. Kherrab-Boukezzata H, Ghemmit-doulache N, Bounoughaz M et al. Electrochemical behavior of zinc anode in acidic zinc electrolyte - influence of lead as an impurity in zinc anodic dissolution. J Fund Appl Sci. 2022;14:391-416. https://doi.org/10.4314/jfas.1142
22. Leidheiser H. Electrical and electrochemical measurements as predictors of corrosion at the metal-organic coating interface. Prog Org Coat. 1979;7(1):79-104. https://doi.org/10.1016/0300-9440(79)80038-7
23. Hai X, Cheng-Man D, Digby M et al. Electrochemical measurements used for assessment of corrosion and protection of metallic materials in the field: A critical review. J Mat Sci Technol. 2022;112:151-183. https://doi.org/10.1016/j.jmst.2021.11.004

24. Cui LF, Chen MX, Huo G et al. FeCo nanoparticles wrapped in N doped carbon derived from Prussian blue analogue and dicyandiamide as efficient oxygen reduction electrocatalysts for Al-air batteries. Chem Eng J. 2020;395:125-158.
25. ISO 2808-2007. Paints and Varnishes-determination of Film Thickness. Classification. ISO. Geneva. 2007.
26. Segall MD, Lindan PJD, Probert MJ et al. First principles simulation: ideas, illustrations and the CASTEP code. J Phys Condens Mat. 2002;14:2717-2744.
27. Tobias H, Soffer A. The immersion potential of high surface electrodes. J Electroanalyt Chem Interfac Electrochem. 1983;148(2):221-232. https://doi.org/10.1016/S0022-0728(83)80398-2
28. Le Pen C, Lacabanne C, Pébère N. Characterisation of water-based coatings by electrochemical impedance spectroscopy. Prog Org Coat. 2003;46:77-83. https://doi.org/10.1016/S0300-9440(02)00213-8
29. O'Donoghue, Michael W, Garrett J et al. Field Performance Versus Laboratory Testing: A Study of Epoxy Tank and Vessel Linings Used in the Canadian Oil Patch. Corrosion. 2003. San Diego. California. 2003.
30. Al-Borno A. Coatings for damp pipe surfaces. Corrosion. 2003:03011. NACE. Houston.Texas. 2003:1-7.
31. Roberge PR. Hand Book of Corrosion Engineering. McGraw-Hill. New York. USA. 2000:863-919.
32. Baeckmann WV, Schwenk W, Prinz W. Hand Book of Cathodic Corrosion Protection. Gulf Professional Publishing. USA. 1997:391-413.
33. Deshpande P, Kolekar A, Bhopale A et al. Impressed current cathodic protection (ICCP) of mild steel in association with zinc-based paint coating. Mat Tod: Proceed. 50:1660-665. https://doi.org/10.1016/j.matpr.2021.09.145